Minimization of acquisition time in short-range free-space optical communication

Jin Wang, Joseph M. Kahn, and Kam Y. Lau

We consider short-range (1–3-km) free-space optical communication between moving parties when covertness is the overriding system performance requirement. To maximize covertness, it is critical to minimize the time required for the acquisition phase, during which the party initiating contact must conduct a broad-field scan and so risks revealing his position. Assuming an elliptical Gaussian beam profile, we show how to optimize the beam divergence angles, scan speed, and design of the raster scan pattern so as to minimize acquisition time. In this optimization, several constraints are considered, including: signal-to-noise ratio, required for accurate bearing detection and reliable decoding; limited receiver bandwidth; limited scanner speed; and beam divergence as limited by the scanner mirror dimensions. The effects of atmospheric turbulence are also discussed. © 2002 Optical Society of America

OCIS codes: 060.0060, 060.4510, 140.3300, 040.1240, 120.5800.

1. Introduction

Free-space optical communication can be made less susceptible to unwanted detection than radio-frequency communication because it is possible to concentrate an optical transmission in a narrow beam aimed toward the intended recipient. Hence free-space optical transmission is an attractive option for covert communication between moving platforms, such as aircraft or ground vehicles. However, the desired covertness may be easily defeated during the acquisition phase of the communication sequence, when at least one party has to perform a broad-field search to acquire the position of the other party, thereby revealing his presence. Moreover, because the optical beam is typically narrow, when the communicating parties are in rapid motion, it may be difficult to maintain a communication link for a significant time interval. Under these conditions, it may be necessary to perform link acquisition repeatedly, increasing the risk of detection. To maximize covertness, it is desirable to achieve acquisition and data transfer in the shortest possible time and for the parties to emit no light until the start of another transmission sequence. In this paper we address the issue of minimizing the acquisition time in short-range links (ranges of order 1 km) between rapidly moving platforms. We show how to minimize this time by the choice of raster scan pattern and by optimization of the beam divergence and scan speed subject to several constraints imposed by hardware and link reliability.

Beam pointing and the acquisition issue in free-space laser communications has been treated in many papers and books, e.g., Refs. 1–7. All those studies considered long-range links, which utilize very narrow beam widths (typically, in the microradian range) and which typically use slow, bulky beam-scanning devices, such as gimballed telescopes driven by servo motors. In those applications, fast acquisition has not typically been as important an issue as reliable, long-term tracking. In contrast, our application involves short-range links between rapidly moving platforms. Hence the beam width may be increased to the milliradian range, and fast, compact beam-scanning devices must be utilized. For the sake of covertness, the minimization of acquisition time is the overriding goal of system design.

The remainder of this paper is as follows. In Section 2 we describe the hardware configuration assumed in our system design. In Section 3 we describe a fast link initiation–acquisition algorithm

J. Wang (wangjin@eecs.berkeley.edu), J. M. Kahn (jmk@eecs.berkeley.edu), and K. Y. Lau (klau@eecs.berkeley.edu) are with the Department of Electrical Engineering and Computer Sciences, University of California, 211 Cory Hall #1722, Berkeley, California 94720.

Received 12 March 2002; revised manuscript received 20 August 2002.

0003-6935/02/367592-11$15.00/0

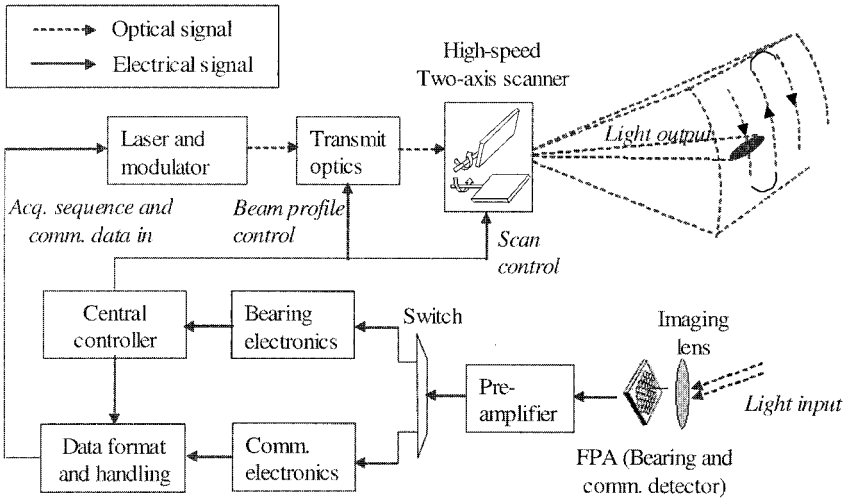

Fig. 1. Example of a short-range free-space optical communication system configuration.

specially designed to exploit this hardware configuration. In Section 4 we analyze the time required for acquisition and describe a procedure to optimize the beam divergence and scan speed to minimize this time. In Section 5 we provide a system design example illustrating our minimization procedure. Then, in Section 6, we discuss the effects of atmospheric turbulence on the acquisition and the design procedure. We present a summary in Section 7.

2. Communication System Configuration

The basic functional components of a point-to-point short-range optical communication system are shown in Fig. 1 (although a system involves at least two communicating parties, only one party is shown in the figure). A high-power, eye-safe laser and a two-axis scanner constitute a scannable light source with an angular field of travel wide enough to cover the whole search field. The scanner is assumed to scan in raster mode, as this mode is readily implemented by use of fast, compact scanners, such as those using mirrors fabricated in microelectromechanical systems technology. Transmit optics, placed between the laser source and the scanner, are used to alter the beam profile to facilitate acquisition. The beam emitted from the scanner has an angular extent of several milliradians, which is narrow enough for short-range optical communication, alleviating the need for a bulky telescope.

As shown in Fig. 1, we use a focal-plane array (FPA) as both a bearing detector and a detector of digital transmissions. The FPA has a field of view sufficiently wide to cover the full search field, which is assumed to be of the order of a radian in each angular dimension. Hence the receiving party need not scan his receiver aperture to acquire the transmitting party, which helps to decrease acquisition time.[7] Furthermore, by use of a large number of pixels, the FPA is able to detect the bearing of the transmitting party with a resolution smaller than the transmitted beam divergence. By virtue of the large number of pixels, each pixel subtends a small enough angle that ambient light noise is negligible compared with thermal noise from the FPA circuits.

The FPA is designed to work in two modes. For purposes of bearing detection, it operates in a "stare" mode, in which all the pixels in the detector array are monitored. In the stare mode the FPA simply detects the presence of an incoming beam and determines which pixel(s) the image falls on (we assume that the image spot size is of the same order as the pixel size and that it typically covers several neighboring pixels simultaneously). To catch the signal whenever it comes, in the stare mode, the FPA must monitor each pixel continuously, with minimal dead time. In stare mode, the FPA operates as follows. Each pixel is coupled to an integrator, which integrates for a fixed exposure interval. At the end of an exposure interval, the output of all integrators are simultaneously sampled and held, and then all integrators are simultaneously reset. The time required to perform the sample–hold–reset operation is negligible compared with the exposure interval. During each exposure interval, the sampled-and-held integrator outputs from the previous exposure interval are read out of the array. The exposure interval is always equal to the time required to read out all the integrator outputs. When we have some prior knowledge of the position of the image in the FPA, only a subset of the integrated pixels needs to be read out, and the integration–readout period can be shortened.

The FPA can be switched electronically to a data-receiving mode, in which the only pixels monitored are those in a small region surrounding the image of the incoming beam. The outputs of these pixels are not integrated but are preamplified and sent to data-detection circuits. Because all the other pixels are deactivated, detector capacitance is reduced, allowing the FPA to serve as a high-speed, low-noise receiver.

Our initiation–acquisition protocol introduced in Section 3 is designed specifically to work with this

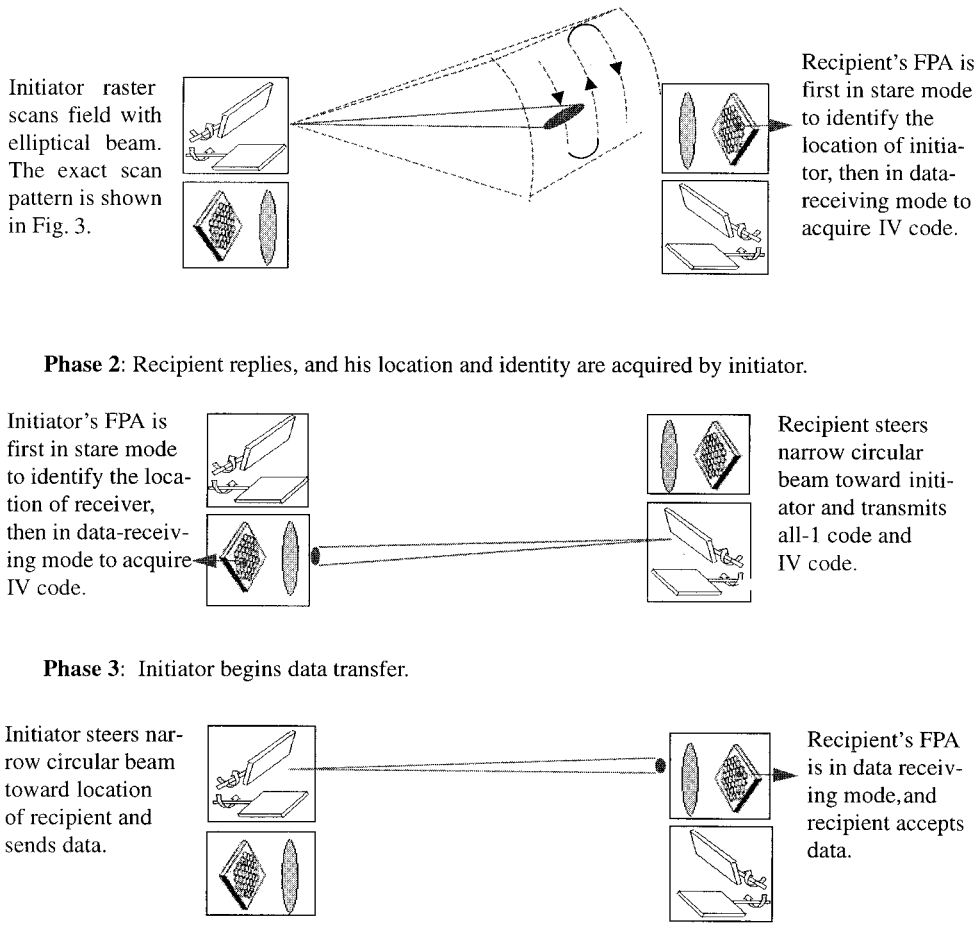

Fig. 2. Link initiation–acquisition protocol. IV code, identity-verifying code.

system configuration by use of a two-axis raster scanner and a dual-mode FPA.

3. Initiation–Acquisition Protocol

The initiation–acquisition protocol is illustrated in Fig. 2. The party initiating the communication is referred to as the initiator, and the other party is called the recipient. During phase 1, the initiator performs a raster scan using an elliptical beam, permitting the recipient to determine the initiator's bearing and identity. During phase 2, the recipient transmits a circular beam to the initiator, allowing the initiator to determine the recipient's bearing and identity. During phase 3, the initiator uses a circular beam to transmit data to the recipient.

A. Phase 1

Both initiator and recipient are in the idle state: Their lasers are turned off, and their FPA receivers are in wide-field stare mode, capable of receiving at any time from any bearing within their respective field of views. The initiator begins scanning a beam over the search field. In general, the beam profile is elliptical; this choice minimizes the time required to complete the initiation–acquisition sequence, as shown in Section 4.

The scanning pattern employed by the initiator is shown in Fig. 3. The entire search field is partitioned into m columns, and each column is covered by n scan paths. In each column the initiator first performs a standard raster scan, transmitting the all-1 code used for bearing detection. After scanning the column, the initiator goes back n paths to the start of the column and scans the column again using a double-looped pattern. In the double-looped pattern, each loop (consisting of two adjacent paths scanned in opposite directions) is scanned with an all-1 code and then immediately scanned again with an identity-verifying (IV) code. In Fig. 3, solid and dashed curves indicate transmission of the all-1 code and the IV code, respectively.

The beam flashes over the recipient exactly three times during phase 1: once during the standard raster scan and twice during the double-looped scan.

When the beam first flashes over the recipient (during the standard raster scan), the all-1 signal illuminates one or more pixel(s) in the recipient's FPA. The FPA, in stare mode, integrates all its pixels and

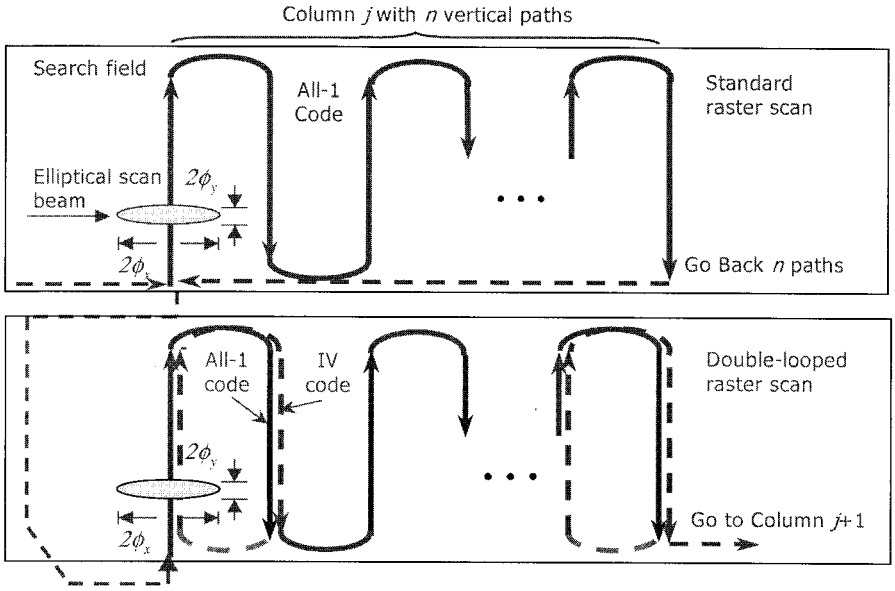

Fig. 3. Scan patterns for the standard raster scan and the double-looped raster scan. The rectangular search field is divided into many columns. Each column contains n vertical paths. In each column the initiator first performs a standard raster scan, transmitting the all-1 code. At the end of this scan, the beam is then moved back n paths, and a double-looped scan is performed, sending the all-1 code and an IV code on alternate loops.

then reads out all pixels and determines which pixel(s) received the all-1 signal. Before the beam flashes over the recipient the second time, the recipient must reconfigure his FPA to stare over a small subset of pixels near the illuminated pixel(s). Because of relative motion between the initiator and the recipient, the subset of pixels must be large enough to include the pixels illuminated when the beam flashes over the recipient the second time. We refer to this process as coarse bearing detection.

When the beam flashes over the recipient a second time, the all-1 signal illuminates one or more pixel(s) in the subset. The pixels within this small subset can be read out rapidly, and the recipient's FPA is rapidly reconfigured to data-receiving mode over the pixel(s) illuminated by the all-1 signal. This process is referred to as fine bearing detection. When the beam flashes over the recipient a third time, the recipient receives and verifies the initiator's IV code.

The advantage of the double-looped scan is that the beam flashes over the recipient two times in rapid succession, so that even when the communication parties are in high-speed movement, the image still falls on the same pixel(s) when the recipient receives the all-1 code and the IV code. This ensures that after the recipient performs fine bearing detection, he activates the correct pixels in data-receiving mode for reception of the initiator's IV code. The image will fall on the same pixel(s) when the recipient receives the all-1 code and the IV code even when the parties are moving at several times the speed of sound, so long as a scanner having a resonant frequency of at least several kilohertz is used.

B. Phase 2

On receiving and verifying the initiator's IV code, the recipient replies by steering a narrow circular beam toward the initiator. The beam should be wide enough to cover the range over which the initiator will move during the readout time of the initiator's FPA. The initiator's FPA, which has remained in the stare mode thus far, acquires the incoming beam from the recipient, determines the recipient's bearing, switches to data-receiving mode, and verifies the IV code from the recipient.

C. Phase 3

Now that the initiator and the recipient have acquired each other's bearings and verified each other's identities, a narrow circular beam is used for high-speed data transfer.

It is worth noting that covertness is least ensured during phase 1, when the initiator transmits a broad, elliptical beam and thus risks announcing his presence. Once the recipient acquires the initiator, the remaining acquisition process and the data transfer can be accomplished by use of narrowly collimated circular beams, minimizing the probability of detection by a third party.

4. Minimization of Acquisition Time

In the protocol described above, the total initiation–acquisition time, T_{acq}, is the sum of the times required for phases 1 and 2. However, there is no scanning required in phase 2, making that phase much shorter than phase 1. Hence, for simplicity, we regard the time required to complete phase 1 as the acquisition time T_{acq}.

As explained in Section 3, the scan paths are di-

vided into columns, and the scan process for each column involves three steps: standard raster scan, going back n paths, and double-looped raster scan. In the following calculations, we neglect the time required to go back n paths. We represent the times required for the standard raster scan and the double-looped scan in one column by τ_s and τ_d, respectively. As before, m is used to represent the total number of columns.

The total time required to perform acquisition over the full rectangular search field shown in Fig. 3 can be expressed as

$$T_{\text{acq}} = m(\tau_s + \tau_d) = m\tau_s + m\tau_d. \quad (1)$$

We note that $m\tau_s$ and $m\tau_d$ are nothing but the times required for the full-field standard raster scan and the full-field double-looped scan, respectively. If we represent these by T_s and T_d, respectively, we can rewrite Eq. (1) as

$$T_{\text{acq}} = T_s + T_d. \quad (2)$$

The times T_s and T_d are associated with two distinct scan modes. To be clear, we will analyze the two scan modes individually and then consider the minimization of the sum of scan times [Eq. (2)]. Accordingly, the analysis will be carried out in four steps. First, in Subsection 4.A we make some preparations for the analysis of two scan modes. We deduce a relationship between beam divergence and scan step, and we introduce two error probabilities used to evaluate bearing detection and identity verification. Then in Subsection 4.B we analyze the standard raster scan. We show how the error probability requirements can be converted into requirements on the signal-to-noise ratio (SNR) of the output signals of the illuminated pixels when there is no atmospheric turbulence, and we obtain an expression for the full-field scan time. In Subsection 4.C we perform a similar analysis for the double-looped scan. Then in Subsection 4.D we discuss the minimization of $T_s + T_d$ under several practical constraints.

A. Preparation for the Analysis of Two Scan Modes

Referring to Fig. 4, we assume that the initiating party must search a field whose angular extent is $\alpha \times \alpha$ along the x and y directions. The initiator transmits an elliptical beam whose divergence is $2\Phi_x \times 2\Phi_y$. To avoid having to change beam profile during scanning, we employ the same beam divergences for both the standard raster scan and the double-looped raster scan. We assume the beam spot has a Gaussian profile in the far field in which the recipient lies and that the principal axes of the beam profile are along the x and y directions.

The beam is raster scanned with a scanner capable of scanning along the x and y directions. Our acquisition algorithm requires the scanner to scan rapidly along the y direction and much more slowly along the x direction. Along the y direction, the round-trip scan time is T_1 during the standard raster scan and T_2 during the double-looped scan.

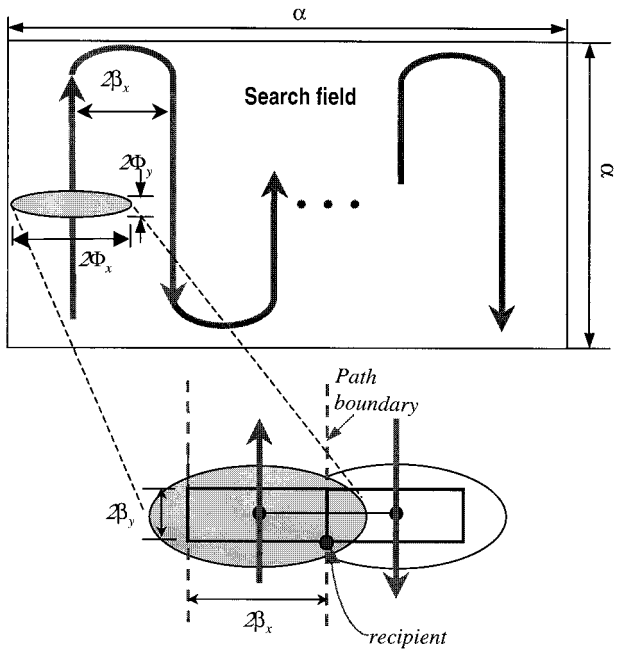

Fig. 4. Scanning geometry during the acquisition process. The rectangle inside the beam is referred as the effective beam spot.

The scan step in the x direction is represented by $2\beta_x$. To calculate the received light power, we consider the worst case from the standpoint of the SNR, which is when the recipient happens to lie on the path boundary, where the received light power is lowest, as shown in Fig. 4. In the particular case of IV code reception during the double-looped scan, we consider the SNR when the recipient lies at the corner of the rectangle of extent $2\beta_x \times 2\beta_y$. This rectangle is referred to as the effective beam spot for the double-looped scan, as we assume that the recipient receives a signal sufficiently strong for decoding IV bits only when he lies within this rectangle.

As the recipient is assumed to lie at the corner of the effective beam spot, the light power received by the recipient is given by

$$P(\Phi_x, \Phi_y, \beta_x, \beta_y) = [2I(\Phi_x, \Phi_y, \beta_x, \beta_y) L_o A_R P_t \cos \Psi]/(\pi d^2), \quad (3)$$

where L_o represents the various optical losses on the path from the initiator's transmitter to the recipient's receiver (in this subsection we neglect the effect of atmospheric turbulence, so these losses are assumed to be fixed), A_R is the area of the receiver lens, Ψ is the angle between the received beam and the lens surface normal, d is the distance between communication parties, P_t is the transmitted laser power, and $I(\Phi_x, \Phi_y, \beta_x, \beta_y)$ is the far-field beam profile. The far-field profile of a Gaussian beam is known to be[8]

$$I(\Phi_x, \Phi_y, \beta_x, \beta_y) = \exp[-2(\beta_x^2/\Phi_x^2 + \beta_y^2/\Phi_y^2)]/(\Phi_x \Phi_y). \quad (4)$$

Because of the monotonic behavior of the exponential function, we can choose the ratios of β_x to Φ_x and

β_y to Φ_y to maximize Eq. (3) by setting $\partial P/\partial \Phi_{x,y} = 0$. The solutions relate the divergences of the *effective* beam spot to those of the elliptical beam spot as

$$\Phi_x = 2\beta_x, \qquad \Phi_y = 2\beta_y. \tag{5}$$

As the total light power P_t is fixed, Eqs. (5) ensure that the light power is most evenly distributed in the effective beam spot.[9] We require these equations to be satisfied in the remainder of Section 4. It is worth noting that during the standard raster scan, the incoming signal is integrated almost continuously as the beam is scanned along the y direction, and it is inappropriate to use the effective beam spot in that case. Therefore we require only $\Phi_x = 2\beta_x$ there.

For both bearing detection and identity verification, we are interested in two types of error event: missed detection (MD) and false alarm (FA). We use their probabilities of occurrence to quantify the performance of bearing detection and identity verification. However, it should be clear that the definitions of these two errors are different for bearing detection and identity verification. During bearing detection, MD happens when the FPA is illuminated, and one or more pixel(s) receive a signal, but the bearing detection circuits fail to register any of these pixel(s). Likewise, during bearing detection, FA happens when the FPA is not illuminated but the bearing detection circuits report that at least one pixel is illuminated. During identity verification, MD happens when the genuine IV code is transmitted by the initiator but the recipient's decoding result indicates that the wrong IV code is received. Likewise, during identify verification, FA happens when the wrong IV code is transmitted but the decoding circuits determine it to be the correct IV code. In the following analysis, we will show that the error probabilities of MD and FA are closely related to the SNR at the receiver in both bearing detection and identity verification.

B. Analysis of the Standard Raster Scan

As explained in Section 3, when the initiator scans in the standard raster mode, the recipient's FPA is in stare mode, and the signal from each pixel is sent to its corresponding integrator. We assume the output of integrator has a Gaussian probability density function $N(\mu_1, \sigma_1^2)$ if the corresponding pixel is illuminated and $N(0, \sigma_1^2)$ if the corresponding pixel is not illuminated. Here the SNR is defined as μ_1^2/σ_1^2. As we pointed out in Section 2, the ambient light noise can be neglected, so that thermal noise is dominant and the noise power σ_1^2 is constant. We set the decision threshold to be h, which means that if the output of any integrator is above h, the bearing detection circuits report that the corresponding pixel was illuminated. To calculate the probability of MD, P_{MD}, we assume that J pixels are equally illuminated at the same time, which generally maximizes P_{MD} except when the SNR is extremely low. Under this assumption, the probability of MD is given by

$$\begin{aligned} P_{\mathrm{MD}} &= [\mathrm{Prob}(U_i < h | \text{pixel } i \text{ illuminated})]^J \\ &= \left[Q\left(\frac{\mu_1 - h}{\sigma_1} \right) \right]^J, \end{aligned} \tag{6}$$

where U_i is the output of the integrator coupled to pixel i and $Q(.)$ is defined as $Q(x) = 1/(\sqrt{2\pi}) \int_x^\infty \exp(-t^2/2)\mathrm{d}t$. To calculate the probability of FA, we consider the complementary case: The FPA is not illuminated, and no pixels are reported illuminated. If we use M to represent the total number of pixels in the FPA, then the probability of FA will be

$$\begin{aligned} P_{\mathrm{FA}} &= 1 - [\mathrm{Prob}(U_i < h | \text{pixel } i \text{ not illuminated})]^M \\ &= 1 - \left[1 - Q\left(\frac{h}{\sigma_1} \right) \right]^M. \end{aligned} \tag{7}$$

Since $Q(.)$ decreases monotonically as its argument increases, if P_{MD} and P_{FA} are required to be less than some given values, we can first determine a minimum required value for h/σ_1 using Eq. (7) to meet the requirement for P_{FA} and then substitute it into Eq. (6) to find a minimum value of μ_1/σ_1 required to meet the requirement for P_{MD}. We observe that the threshold h can be set at will and that μ_1/σ_1 is simply the square root of the SNR at the output of the integrator at an illuminated pixel. Thus the requirements for P_{MD} and P_{FA} are converted into a minimum required value of the SNR during bearing detection, referred to as SNR_1. In the following discussions, we consider the required value of SNR_1 instead of considering required values of P_{MD} and P_{FA}.

To compute the SNR, using Eqs. (3)–(5), we can determine the optical power received by the recipient at the path boundary:

$$\begin{aligned} P_s(\Phi_x, \Phi_y, \beta_x, \theta_y) = \frac{2L_o A_R P_t \cos \Psi}{\pi d^2 \Phi_x \Phi_y} \exp\left(-\frac{1}{2} \right) \\ \times \exp\left(-\frac{2\theta_y^2}{\Phi_y^2} \right), \end{aligned} \tag{8}$$

where θ_y represents the vertical angular distance between the recipient and the beam-spot center. During the scanning, θ_y keeps changing. Considering that the beam divergence is much less than the field angular extent, we can assume that θ_y changes from $-\infty$ to ∞ for the following integration. When the beam flashes over the recipient with angular speed ω, the total optical energy received by the FPA is $\int_{-\infty}^{\infty} (P_s/\omega)\mathrm{d}\theta_y$, and the output of the integrator coupled to one illuminated pixel (among the J equally illuminated) has an SNR of

$$\mathrm{SNR} = \left(\int_{-\infty}^{\infty} \frac{RP_s}{J\omega} \, \mathrm{d}\theta_y \right)^2 \Big/ (N_0 T_{\mathrm{int}}), \tag{9}$$

where R is the detector responsitivity, N_0 is the (one-sided) power spectral density of the receiver noise

(which we assume is white Gaussian), and T_{int} is the integration time. During the standard raster scan, all the pixels in the FPA are sampled, so T_{int} is equal to the readout period of the FPA. The calculation of the signal energy in Eq. (9) is straightforward; for calculation of the noise component, see Ref. 10. For a raster scanner, assuming the scan beam moves with a constant speed, ω can be readily expressed in terms of the field angular extent α, and the round-trip scan time T_1 as $\omega = (2\alpha)/T_1$. Performing the integration in Eq. (9), we obtain

$$\text{SNR} = \kappa(T_1^2/\Phi_x^2), \tag{10}$$

where $\kappa \equiv \pi/(2N_0T_{\text{int}})[RL_oA_RP_t \cos \Psi/(\pi d^2 e^{1/2}\alpha J)]^2$. Note that in this paper the letter e represents Euler's constant (2.718 . . .).

With the scan step equal to $2\beta_x$, i.e., Φ_x, the time required for the full-field standard raster scan can be expressed as

$$T_s = \alpha T_1/(2\Phi_x). \tag{11}$$

Equation (10) shows T_1 is proportional to Φ_x; hence Eq. (11) can be rewritten as

$$T_s = (\alpha/2)\sqrt{\text{SNR}/\kappa}. \tag{12}$$

We note that T_s is independent of beam divergences Φ_x and Φ_y. In the following analysis, this fact enables us to determine the beam divergences in minimizing double-looped scan time and to assume the same values of beam divergences for the standard raster scan.

C. Analysis of Double-Looped Raster Scan

Recalling the initiation–acquisition protocol, when the initiator scans in the double-looped raster mode, the recipient first locates the pixels that are receiving the all-1 code and then activates only these pixels to receive the IV code. In the receiving of the IV code, we assume that maximal-ratio combining[11] is used to combine the signals from the multiple illuminated pixels to maximize the SNR. As the IV code inevitably includes 0 and 1 bits, we assume the sampled output of the combining circuits has a Gaussian probability density function $N(\mu_2, \sigma_2^2)$ if the received bit is 1 and $N(0, \sigma_2^2)$ if it is 0. Similar to before, we define the SNR as μ_2^2/σ_2^2. Assuming the decision threshold is set at $\mu_2/2$ and symbol-by-symbol detection is performed, the bit-error probability P_b is[10]

$$P_b = Q(\sqrt{\text{SNR}}/2). \tag{13}$$

The bit-error probability for all the bits in the received IV code is assumed to be the same. If the IV code is N bits long and the IV code must be received without error for identity verification, then the error probability of MD can be expressed in terms of P_b:

$$P_{\text{MD}} = 1 - (1 - P_b)^N. \tag{14}$$

To compute the error probability of FA, we assume that each wrong IV code (with 1, 2, . . . , N bits in error) occurs with equal probability $1/2^N$, thus obtaining

$$P_{\text{FA}} = \frac{1}{2^N - 1}\left[\sum_{i=1}^{N}\binom{N}{i}P_b^i(1 - P_b)^{N-i}\right] = \frac{P_{\text{MD}}}{2^N - 1}. \tag{15}$$

As N is usually a large integer, we see that P_{FA} is much lower than P_{MD}. If the probabilities of MD and FA are required to be less than some given values, according to the behavior of the $Q(.)$ function, we can easily determine minimum required values of the SNR using Eqs. (13)–(15). Thus the requirements for the probabilities of MD and FA in IV code reception can be converted into a SNR required for IV code detection, denoted by the symbol SNR_2.

In Subsection 4.A we have maximized the received light power in IV code reception. Substituting Eqs. (4) and (5) into Eq. (3) yields the light power

$$P_d = (2L_oA_RP_t \cos \Psi)/(\pi e d^2 \Phi_x \Phi_y), \tag{16}$$

and, accordingly, the SNR is given by

$$\text{SNR} = (R^2P_d^2T)/(JN_0) = \chi T/(\Phi_x^2\Phi_y^2), \tag{17}$$

where T is the bit interval of IV code; R, J, N_0 are defined as before; and $\chi \equiv (2RL_oA_RP_t \cos \Psi)^2/(\pi^2e^2d^4JN_0)$. To obtain the above SNR, we have utilized the optimum receiver for the additive white Gaussian noise channel.[10]

Recalling that the scan step is Φ_x and the round-trip scan time is T_2, we can express the time required for the full-field double-looped raster scan as

$$T_d = \alpha T_2/\Phi_x. \tag{18}$$

D. Minimization of Acquisition Time

Now we wish to minimize $T_{\text{acq}} = T_s + T_d$ by optimizing the beam divergences Φ_x, Φ_y, the round-trip scan times T_1, T_2, and the IV code bit interval T subject to the following constraints.

(i) SNR requirements: $\text{SNR} \geq \text{SNR}_1$ for the standard raster scan and $\text{SNR} \geq \text{SNR}_2$ for the double-looped raster scan, where SNR_1 and SNR_2 are the minimum values of the SNR required for bearing detection and IV code reception, respectively.

(ii) Scanner speed limit: $T_1 \geq T_y$ and $T_2 \geq T_y$, where T_y is the minimum round-trip scan time that can be achieved by the scanner.

(iii) Receiver bandwidth limit: $T \geq 1/B_{\text{rec}}$, where B_{rec} is the receiver electrical bandwidth.

(iv) Diffraction limit imposed by the scanner mirror dimensions:

$$\Phi_x \geq \Phi_{x\min} \equiv \lambda/(\pi r), \qquad \Phi_y \geq \Phi_{y\min} \equiv \lambda/(\pi r), \tag{19}$$

where λ is the laser wavelength and r is the scanner mirror radius (assuming the mirror is circular). To determine $\Phi_{x\min}$ and $\Phi_{y\min}$, we assume the near-field beam width w_x, w_y should not exceed the mirror ra-

dius r in order to reduce power loss during reflection[12] and utilize the known relation between the near-field Gaussian beam width and the beam divergence given by[13] $\Phi_y = \lambda/(\pi w_x)$ and $\Phi_x = \lambda/(\pi w_y)$.

(v) Identical beam divergences are employed during the standard raster scan and the double-looped scan.

In Subsection 4.B Eq. (12) gives us the full-field standard raster scan time. Examining Eq. (12), we see that T_s depends only on the parameters associated with the standard raster scan, i.e., SNR_1 and T_1, which implies that T_s is independent of T_d. This fact allows us to minimize T_{acq} by minimizing T_s and T_d separately, which greatly simplifies our analysis. Because T_s is independent of beam divergences, as we pointed out at the end of Subsection 4.B, we can choose the beam divergences to minimize T_d and then use the same values for the standard raster scan, thus satisfying constraint (v).

Substituting the SNR requirement SNR_1 into Eq. (12), we obtain the minimum value of T_s as follows:

$$T_{s\min} = (\alpha/2)\sqrt{\mathrm{SNR}_1/\kappa}. \tag{20}$$

We note that to achieve this minimum we must satisfy the equation $T_1 = \Phi_x\sqrt{\mathrm{SNR}_1/\kappa}$, and, because of the scanner speed limit, we must satisfy the follow inequality:

$$\Phi_x\sqrt{\mathrm{SNR}_1/\kappa} \geq T_y. \tag{21}$$

Note that Φ_x is determined by consideration of the double-looped scan. In our application, we envision using fast scanners, such as those made of microelectromechanical mirrors, so that T_y is typically small enough to easily satisfy inequality (21), as we will demonstrate in Section 5. In the case that T_y is so large that inequality (21) cannot be satisfied with the value of Φ_x determined for the double-looped scan, we must increase the value of Φ_x until inequality (21) is satisfied. In the remainder of our analysis, we will assume that T_y is small enough to permit T_s to be minimized by employing the beam divergences determined by the double-looped scan.

For the minimization of T_d, all the constraints listed above need to be considered. In the following analysis, first, we ignore the constraint from the diffraction limits of the scanner mirrors and convert the first three constraints into three lower bounds on the IV bit interval T; then we will substitute these lower bounds into the expression for T_d and minimize it. Finally, we will revise our results taking account of the diffraction limits.

As the SNR during IV code reception is required to exceed SNR_2, using Eq. (17) we obtain the first constraint on T:

$$T \geq \Phi_x{}^2\Phi_y{}^2(\mathrm{SNR}_2/\chi). \tag{22}$$

For the recipient to receive the N-bit-long IV code correctly, the beam must illuminate the recipient for a duration of at least NT. We have assumed that only when the recipient lies inside the effective beam spot with divergence $2\beta_x \times 2\beta_y$ can he receive the signal, so we have $2\beta_y/\alpha(T_2/2) = NT$. The constraint of scanner speed limit requires $T_2 \geq T_y$, which turns into the second constraint on T:

$$T \geq \Phi_y T_y/(2N\alpha). \tag{23}$$

The third constraint on T is imposed by the bandwidth limit, which can be written as

$$T \geq 1/B_{\mathrm{rec}}. \tag{24}$$

With three lower bounds on T given by inequalities (22)–(24), Eq. (18) can be converted into an inequality describing the double-looped scan time:

$$T_d \geq 2N\alpha^2 \max\left(A\Phi_x\Phi_y, \frac{B}{\Phi_x}, \frac{C}{\Phi_x\Phi_y}\right), \tag{25}$$

where $A = \mathrm{SNR}_2/\chi$, $B = T_y/2N\alpha$, and $C = 1/B_{\mathrm{rec}}$.

Inequality (25) can be satisfied with equality if $\Phi_x\Phi_y = \sqrt{C/A}$ and $\Phi_y \leq C/B$, and we can obtain the minimum value of T_d as

$$T_{d\min} = 2N\alpha^2\sqrt{AC}. \tag{26}$$

If we define $\Phi_{y\max} \equiv C/B$, then for T_d to achieve the minimum value given by Eq. (26) we must have

$$\Phi_y \leq \Phi_{y\max}. \tag{27}$$

We now consider the effect of the diffraction limits. Observing inequalities (19) and (27), we can see that if $\Phi_{y\min} \leq \Phi_{y\max}$, then both inequalities are satisfied when Φ_y takes any value between $\Phi_{y\min}$ and $\Phi_{y\max}$. We refer to this as the non-diffraction-constrained case. If, however, $\Phi_{y\min} > \Phi_{y\max}$, then inequality (27) cannot be satisfied. In this situation, which we call the diffraction-constrained case, it is easily shown that, when $\Phi_y = \Phi_{y\min}$, T_d can be minimized and takes on a value given by

$$T_{d\min} = 2N\alpha^2\sqrt{AB\Phi_{y\min}}. \tag{28}$$

In Table 1, for the double-looped scan, we list the optimized values of Φ_x, Φ_y, and T and the minimized value of $T_{d\min}$ for the two cases. In Table 2, for the standard raster scan, we list the optimized value of T_1 and the minimized value $T_{s\min}$. Recall that to simplify implementation, we choose the same values of Φ_x and Φ_y for the standard raster scan as for the double-looped scan.

We note that in our analysis of the double-looped scan we considered the SNR required for IV code reception, but not for fine bearing detection. We did so considering that, in practice, fine bearing detection imposes looser constraints on beam divergence because the recipient does not need to check the contents of the all-1 code and the number of pixels monitored is extremely limited during fine bearing detection. We will demonstrate this fact in Section 5.

Before closing this subsection, we summarize our optimization procedure as follows.

Table 1. Double-Looped Raster Scan: Optimal Beam Divergences, Bit Interval, and Minimized Full-Field Scan Time[a]

Case	Φ_y	Φ_x	T	$T_{d\min}$
Case 1: $\Phi_{y\min} \le \Phi_{y\max}$ (non-diffraction-constrained)	$\Phi_{y\min} \sim \Phi_{y\max}$	$\frac{\sqrt{C/A}}{\Phi_y}$	C	$2N\alpha^2\sqrt{AC}$
Case 2: $\Phi_{y\min} > \Phi_{y\max}$ (diffraction-constrained)	$\Phi_{y\min}$	$\frac{\sqrt{B/A}}{(\Phi_{y\min})^{1/2}}$	$B\Phi_{y\min}$	$2N\alpha^2\sqrt{AB\Phi_{y\min}}$

[a]Note that $\Phi_{y\min} = \lambda/\pi r$, $\Phi_{y\max} = C/B$. The round-trip scan time $T_2 = 2NT\alpha/\Phi_y$ for both cases.

1. Minimizing T_d

(i) Calculate SNR_2 according to the specified requirements for the probabilities of MD and FA in IV code reception.

(ii) Write down three constraints on T, i.e., inequalities (22)–(24), and obtain the parameters A, B, and C.

(iii) Compute values of $\Phi_{y\max}$ and $\Phi_{y\min}$.

(iv) Depending on the relationship between $\Phi_{y\max}$ and $\Phi_{y\min}$, determine Φ_x, Φ_y, T, T_2, and $T_{d\min}$ by following Table 1.

2. Minimizing T_s

(i) Using specified requirements for the probabilities of MD and FA during bearing detection, compute SNR_1 by use of Eqs. (6) and (7). Also calculate κ.

(ii) Following Table 2, determine round-trip scan time T_1 and $T_{s\min}$.

5. Design Example

In this section we present a design example to illustrate the optimization procedure described above. We assume that during link setup, the search field angular extent is $\alpha = 1$ rad, the link range is $d = 3$ km, the transmit power is $P_t = 5$ W, the laser wavelength is 1.55 μm, Ψ is approximately 0.5 rad, the receiver noise power density is $N_0 = 0.96 \times 10^{-23}$ A^2/Hz, $R = 1$ mA/mW, the receiver lens area is $A_R = 231$ mm^2, and the receiver maximum bandwidth is $B_{\mathrm{rec}} = 1$ GHz. The FPA is composed of square pixels, and, consequently, we make the worst-case assumption that the signal is divided among $J = 4$ pixels. We take the loss factor to be $L_o = 0.48$. Using these parameters, we obtain $\chi = 4.17$. The IV code length is selected to be $N = 50$ bits.

We assume that during IV code reception, the probabilities of MD and FA must not exceed 10^{-3}. Using Eqs. (13)–(15), we obtain the required SNR, $\mathrm{SNR}_2 = 68$, which is sufficient to achieve a bit-error probability of 2×10^{-5}. We also obtain $A = 16$ and $C = 10^{-9}$.

We assume the use of microelectromechanical scanners characterized by $T_y = 200$ μs and a mirror diameter of 1 mm. We then obtain $B = 2 \times 10^{-6}$, $\Phi_{y\max} = 0.5 \times 10^{-3}$ rad, and $\Phi_{y\min} = 1 \times 10^{-3}$ rad. Comparing the values of $\Phi_{y\max}$ and $\Phi_{y\min}$, we determine that this situation corresponds to the diffraction-constrained case. Using Table 1, we obtain optimum values for beam divergences, the bit interval, and the round-trip scan time: $\Phi_x = 11$ mrad, $\Phi_y = 1$ mrad, $T = 2 \times 10^{-9}$ s, $T_2 = 200$ μs, and $T_{d\min} = 18$ ms. Note that the optimized beam profile is far from circular.

We now compute the round-trip scan time for the standard raster scan. Assuming we have a FPA with 500×500 pixels and both the probabilities of MD and FA for bearing detection are required to be less than 10^{-3}, then using Eqs. (6) and (7) we set $h/\sigma_1 = 5.8$ and obtain the requirement that $\mu_1/\sigma_1 \ge 6.7$. Thus the required value of SNR for coarse bearing detection, SNR_1, is approximately 45. The integration time T_{int} is equal to the readout period of the FPA, which we assume is 250 μs (the readout rate is 1 pixel/ns). All other parameters in the expression for κ take on the same values as for the double-looped scan, so that $\kappa = 1800$. Using Table 2, we obtain $T_1 = 1.8$ ms and $T_{s\min} = 79$ ms. We note that $T_{s\min}$ is much longer than $T_{d\min}$ because of the long readout time of the FPA.

Having determined values of Φ_x, SNR_1, κ, and T_1, we can verify that inequality (21) is fully satisfied, which justifies our using beam divergences optimized for the double-looped scan during the standard raster scan.

Because $T_{d\min} = 18$ ms and $T_{s\min} = 79$ ms, the maximum acquisition time is $T_{\mathrm{acq}} = 97$ ms.

Using this design example, we can validate an earlier assumption that even when the parties are moving rapidly, an extremely limited number of pixels need to be monitored during fine bearing detection. Let us assume that the relative speed is as high as Mach 2 (approximately 660 m/s), so that the relative angular speed is approximately 0.2 rad/s. As the round-trip standard raster scan time has exceeded the readout time of the FPA, only two vertical paths can be included in each column, and the time interval

Table 2. Standard Raster Scan: Beam Divergences, Optimal Value of Round-Trip Scan Time, and Minimized Full-Field Scan Time

Φ_y	Φ_x	T_1	$T_{s\min}$
Same value as in double-looped scan	Same value as in double-looped scan	$\left(\frac{\mathrm{SNR}_1}{\kappa}\right)^{1/2}\Phi_x$	$\left(\frac{\mathrm{SNR}_1}{\kappa}\right)^{1/2}\frac{\alpha}{2}$

between coarse bearing detection and fine bearing detection is less than the round-trip raster scan time of 1.8 ms. During such a short time, the change in bearing is less than 0.4 mrad. Recalling that the image size is of the same order as the pixel size and that each pixel subtends approximately 2 mrad, we can conclude that not more than 3×3 pixels need to be watched during fine bearing detection. It is not difficult for the recipient to monitor this small number of pixels during fine bearing detection, and therefore fine bearing detection places much looser constraints on beam divergences and scan speed than those determined near the end of Subsection 4.D. Even when the link distance becomes less than 3 km and the bearing changes more rapidly, the number of pixels monitored by the recipient during fine bearing detection is still small.

6. Effect of Atmospheric Turbulence

In this section we study the influence of atmospheric turbulence on the acquisition process and show how to modify the optimization procedure to take account of turbulence. Turbulence leads to random fluctuations of the refractive index, which can cause spreading of the beam beyond that caused by diffraction, wander of the beam centroid, change of angle of arrival, and fluctuations in the irradiance of the received beam. In principle, all of these can affect the acquisition process.

In short-range links that use milliradian beam widths, when atmospheric turbulence is not strong, beam spreading, beam wander, and change of angle of arrival are not significant. For example, assuming moderate turbulence with refractive-index structure parameter $C_n^2 = 10^{-15}$, 1.55-μm wavelength, and 3-km link distance, we can apply the Rytov approximation in analyzing beam propagation.[14] We find that in the presence of turbulence the long-term beam radius is enlarged by only 10^{-4} (i.e., by a factor $1 + 10^{-4}$) and that the standard deviation of the beam angular displacement is 0.01 mrad, which is negligible compared with the beam divergence of 1 mrad. The change of angle of arrival is even smaller, and its standard deviation is several orders of magnitude smaller than the receiver's bearing resolution.

The effect of turbulence-induced irradiance fluctuations on the detection process warrants further attention. We first consider the reception of the IV code, as this determines the beam divergence. During a 1 bit, the received intensity is a random variable that, for weak turbulence, is known to follow the log-normal distribution[15]:

$$p(i) = \frac{1}{\sqrt{2\pi}\sigma_l i} \exp\left[-\frac{1}{2\sigma_l^2} \left(\ln i + \frac{1}{2}\sigma_l^2 \right)^2 \right], \quad (29)$$

where $i = I/\langle I \rangle$, I is the 1-bit intensity, and σ_l^2 is the variance of the log-intensity fluctuations. Thus the bit-error probability must be modified from Eq. (13), becoming

$$P_b = \frac{1}{2}\left\{ \int_0^\infty Q[(i - i_{\text{th}})\sqrt{\langle \text{SNR} \rangle}]p(i)\mathrm{d}i + Q(i_{\text{th}}\sqrt{\langle \text{SNR} \rangle}) \right\}, \quad (30)$$

where i_{th} is the optimized threshold, and $\langle \text{SNR} \rangle$ is the average SNR. In the absence of turbulence, $\langle \text{SNR} \rangle$ is equal to the fixed SNR given by Eq. (17). In Eq. (30) the first and second terms are the bit-error probabilities for 1 and 0 bits, respectively. Now we can determine the minimum allowable value of $\langle \text{SNR} \rangle$ based on the required bit-error probability P_b. For example, in the design example of Section 5, from the error probabilities of MD and FA we found the requirement that $P_b \leq 2 \times 10^{-5}$. Thus, if we assume moderate turbulence with $C_n^2 = 10^{-15}$, using Eq. (30), we find that the minimum allowable $\langle \text{SNR} \rangle$, still referred to as SNR_2, must be increased by approximately 10 dB to achieve the required value of P_b. Once we determine SNR_2, the rest of the optimization procedure will be exactly as described previously, and we find that the optimum beam divergence is 1 mrad $\times$ 4 mrad instead of 1 mrad $\times$ 11 mrad. The divergence in the x direction has been reduced to increase the received light intensity, allowing the required value of P_b to be achieved in the presence of turbulence. As a result of this change, the scan time for the double-looped scan is increased from 18 to approximately 57 ms.

We now consider reception of the all-1 code. The value of P_{FA} is unaffected by turbulence, but turbulence does affect computation of P_{MD}. Assuming the same values of link distance d and wavelength λ as in Section 5, we can estimate the correlation length of turbulence intensity fluctuations to be $d_0 \approx \sqrt{\lambda d} = 68$ mm. The component of the relative velocity between the air mass and the beam path that lies perpendicular to the beam path, denoted by $v_\perp$, can range from several tens to several hundreds of meters per second. We can estimate the correlation time of turbulence intensity fluctuations[16] as $\tau_0 \approx d_0/v^\wedge$. We conclude that τ_0 lies between approximately 100 and 1 ms. During reception of the all-1 code, the beam flashes over the recipient for a duration of approximately 1 μs, which is much shorter than τ_0. Therefore the instantiation of the intensity fluctuation can be considered constant while the beam flashes over the recipient, and the value of the integrator output μ_1 appearing in Eq. (6) can be considered a log-normal random variable. To compute P_{MD}, we modify Eq. (6) as follows:

$$P_{\text{MD}} = \left[\int_0^\infty Q(i\sqrt{\langle \text{SNR} \rangle} - h/\sigma_1)p(i)\mathrm{d}i \right]^J, \quad (31)$$

where i is the normalized light intensity and $\langle \text{SNR} \rangle$ is the average SNR for all-1 code reception, given by Eq.

(10). For the system parameters of Section 5, and assuming $C_n^2 = 10^{-15}$, using Eq. (31), we find that the minimum allowable value of $\langle \mathrm{SNR} \rangle$ in all-1 code reception, still referred as SNR_1, must be increased from 45 to 83. This increase of SNR_1 requires the full-field scan time for the standard raster scan to increase from 79 to 107 ms. Finally, summing the times required for the standard raster scan and the double-looped scan, we find the total acquisition time in the presence of turbulence to be approximately 164 ms, a 70% increase from the 96 ms in the absence of turbulence.

In the above, we have considered only the case of moderate turbulence and weak fluctuations. In the case of strong turbulence, the log-normal distribution must be modified, e.g., to the gamma–gamma distribution.[17] Other than replacement of the distribution, the analysis remains identical to that given above.

Aside from simply decreasing the beam divergence to increase the received intensity, other techniques can be used to combat turbulence, including adaptive optics, diversity reception, and various detection techniques.[16] If any of these approaches is taken, the only portion of the optimization procedure that must be modified is calculation of the minimum average SNR required to achieve the required probabilities of FA and MD. Once the SNR requirement is determined, the rest of the optimization procedure remains as described above.

7. Summary

We have proposed a simple procedure for optimizing beam divergences and scan speed to minimize acquisition time in covert short-range free-space optical communication. In this optimization, we have considered several constraints: the receiver SNR requirement for accurate bearing detection and reliable decoding of the IV code, scanner speed limit, receiver bandwidth limit, and scanner mirror diffraction limit.

Assuming a raster scan mode and a Gaussian beam profile, we find that the acquisition time is generally minimized by use of an elliptical beam whose minor axis lies parallel to the direction of fast scanning. In a design example, we showed that the elliptical beam profile may have a high eccentricity. We showed that in our application the majority of the acquisition time is typically spent on bearing detection even when a FPA with a high frame rate is used. This implies that, to further minimize the acquisition time, a faster bearing detection device with wide field of view would need to be developed.

In a typical scenario with a 1 rad $\times$ 1 rad search field, 3-km link distance, and 200-μs minimum round-trip scan time (i.e., maximum scan frequency of 5 kHz), the acquisition time is minimized by use of an 11 mrad $\times$ 1 mrad beam profile. The maximum acquisition time can be reduced to approximately 100 ms.

We also considered the effects of atmospheric turbulence on the optimization of the acquisition procedure. In the presence of turbulence, the optimization procedure is basically unchanged, except for the details of calculating the required SNR for all-1 code and IV code reception. Atmospheric turbulence typically forces us to reduce the beam divergence and increase the acquisition time.

This research has been supported by the Defense Advanced Research Projects Agency, Steered Agile Beam Program under contract DAAH01-00-C-0089. The authors thank the anonymous reviews for suggesting several improvements to the paper.

References

1. I. M. Teplyakov, "Acquisition and tracking of laser beams in space communications," Acta Astron. **7,** 341–355 (1980).
2. R. M. Gagliardi and S. Karp, *Optical Communications* (Wiley, New York, 1976).
3. J. M. Lopez and K. Yong, "Acquisition, tracking, and fine pointing control of space-based laser communication system," in *Control and Communication Technology in Laser Systems*, K. Yong, ed., Proc. SPIE **295,** 100–114 (1981).
4. S. G. Lambert and W. L. Casey, *Laser Communications in Space* (Artech House, Boston, Mass., 1995).
5. E. S. Clarke and H. D. Brixey, "Acquisition and tracking system for a ground-based laser communication receiver terminal," in *Control and Communication Technology in Laser Systems*, K. Yong, ed., Proc. SPIE **295,** 162–169 (1981).
6. R. B. Deadrick, "Design and performance of a satellite laser communications pointing system," Adv. Astronaut. Sci. **57,** 155–166 (1985).
7. M. Scheinfeild, N. S. Kopeika, and R. Melamed, "Acquisition system for microsatellites laser communication in space," in *Free-Space Laser Communication Technologies XII*, G. S. Mecherle, ed., Proc. SPIE **3932,** 166–175 (2000).
8. A. Yariv, *Introduction to Optical Electronics*, 2nd ed. (Holt, Rinehart and Winston, New York, 1976).
9. J. D. Barry and G. S. Mecherle, "Beam pointing error as a significant design parameter for satellite-borne free-space optical communication systems," Opt. Eng. **24,** 1049–1054 (1985).
10. J. G. Proakis, *Digital Communications*, 3rd ed. (McGraw-Hill, New York, 1995).
11. P. Djahani and J. M. Kahn, "Analysis of infrared wireless links employing multi-beam transmitters and imaging diversity receivers," IEEE Trans. Commun. **48,** 2077–2088 (2000).
12. A. L. Bloom, *Gas Lasers* (Wiley, New York, 1968).
13. B. E. A. Saleh and M. C. Teich, *Fundamentals of Photonics* (Wiley, New York, 1991).
14. L. C. Andrews and R. L. Phillips, *Laser Beam Propagation through Random Media* (SPIE Optical Engineering Press, Bellingham, Wash., 1998).
15. C. C. Davis and I. I. Smolyaninov, "Effect of atmospheric turbulence on bit-error rate in an on-off-keyed optical wireless system," in *Free-Space Laser Communication and Laser Imaging*, D. G. Voelz and J. C. Ricklin, eds., Proc. SPIE **4489,** 126–137 (2002).
16. X. Zhu and J. M. Kahn, "Free-space optical communication through atmospheric turbulence channels," IEEE Trans. Commun. **50,** 1293–1300 (2002).
17. L. C. Andrews and R. L. Phillips, "Impact of scintillation on laser communication systems: recent advances in modeling," in *Free-Space Laser Communication and Laser Imaging*, D. G. Voelz and J. C. Ricklin, eds., Proc. SPIE **4489,** 23–34 (2002).